Electric field gradients in *s*-, *p*-, and *d*-metal diborides and the effect of pressure on the band structure and T_c in MgB_2

N. I. Medvedeva,[1,2] A. L. Ivanovskii,[1] J. E. Medvedeva,[2,3] A. J. Freeman,[2] and D. L. Novikov[4]
[1]*Institute of Solid State Chemistry, Ekaterinburg, Russia*
[2]*Department of Physics and Astronomy, Northwestern University, Evanston, Illinois 60208-3112*
[3]*Institute of Metal Physics, Ekaterinburg, Russia*
[4]*Arthur D. Little, Inc., Cambridge, Massachusetts 02140*
(Received 18 April 2001; published 27 December 2001)

Results of full-potential linear muffin-tin orbital generalized gradient approximation calculations of the band structure and boron electric field gradients (EFG's) for the new medium-T_c superconductor MgB_2 and related diborides MB_2, M=Be, Al, Sc, Ti, V, Cr, Mo, and Ta are reported. The boron EFG variations are found to be related to specific features of their band structure and particularly to the M-B hybridization. The strong charge anisotropy at the B site in MgB_2 is completely defined by the valence electrons—a property which sets MgB_2 apart from other diborides. The boron EFG in MgB_2 is weakly dependent on applied pressure: the B *p*-electron anisotropy increases with pressure, but it is partly compensated by the increase of core charge asymmetry. The concentration of holes in bonding σ bands is found to decrease slightly from 0.067 to 0.062 holes/B under a pressure of 10 GPa. Despite a small decrease of $N(E_F)$, the Hopfield parameter increases with pressure and we believe that the main reason for the reduction under pressure of the superconducting transition temperature T_c is the strong pressure dependence of phonon frequencies, which is sufficient to compensate for the electronic effects.

DOI: 10.1103/PhysRevB.65.052501 PACS number(s): 74.72.−h

Recently, Akimitsu and Nagamatsu *et al.*[1] reported the discovery of medium-T_c superconductivity (MTSC) with T_c of about 39 K in magnesium diboride (MgB_2) with a simple composition and crystal structure (AlB_2-type, space group $P6/mmm$, $Z=1$). Band structure calculations showed[2–7] that the MTSC in MgB_2 can be attributed to a strong electron-phonon coupling, a rather high density of states from two-dimensional (2D) (in-plane) metallic boron $\sigma(p_{x,y})$ bands at E_F and the existence of $p_{x,y}$-band holes. By now, a number of studies have been performed with NMR,[8–10] which is a very powerful technique for investigating the properties of MgB_2. The measured quadrupole interaction is determined by the value of the electric field gradient (EFG), which is directly related to the charge distribution around the nucleus. Thus theoretical EFG studies are important in order to give a reliable interpretation of the experimental data based on the electronic structure.

The EFG at the boron site in MgB_2 was found experimentally to be much larger than those for *d*-diborides (Table I). As seen from Table I, the variation in EFG for diborides covers two orders of magnitude and shows trends which cannot be explained by the crystal structure changes. For example, these EFG's in AlB_2 and TiB_2 differ by almost 3 times, but their lattice parameters *a* and *c* are approximately the same and, vice versa, equal EFG's were obtained in BeB_2 and MgB_2, for which the lattice parameters have the largest differences among diborides under consideration. No attempts were made previously to relate the EFG changes to the peculiarities of electronic structure.

In this paper, we present results of first-principles full-potential linear muffin-tin orbital generalized gradient approximation[11] (FLMTO-GGA) calculations (within the GGA for the exchange correlation potential) of the electronic structure and EFG's at the boron site for MgB_2 and other *s*-, *p*-, *d*-diborides. We compare the calculated EFG's with the experimental and other theoretical data and explain the EFG variation based on the anisotropy of boron $2p$ occupancies. The pressure dependence of the EFG, which is very sensitive to the charge distribution, represents a good test for the anisotropy study. The experimental and theoretical data on the electronic and elastic behavior of MgB_2 under pressure are contradictory: it was found to be nearly isotropic,[12,13] anisotropic,[14] or strong anisotropic.[15,16] We simulated the pressure effect on the band structure of MgB_2 and estimated the changes in the EFG, boron *p*-occupancies, hole concen-

TABLE I. Theoretical and experimental boron EFG, V_{zz} (in 10^{21} V/m^2), for *s*-, *p*-, and *d*-diborides.

Diboride	V_{zz}^{el}	V_{zz}^{lat}	V_{zz}	$\lvert V_{zz}^B\rvert$[a]	$\lvert V_{zz}^B\rvert$ Expt.
MgB_2	−1.94	0.06	−1.88		1.69[b]
MgB_2[e]	−2.00	0.10	−1.90		
BeB_2	−2.43	0.33	−2.10		
AlB_2	−1.17	0.18	−0.99		1.08[c]
ScB_2	−0.75	0.13	−0.60		
TiB_2	−0.66	0.31	−0.35	0.38	0.37[d]
VB_2	−0.76	0.38	−0.38	0.39	0.43[d]
CrB_2	−1.01	0.42	−0.59	0.60	0.63[d]
MoB_2	−0.55	0.32	−0.23	0.22	0.23[d]
TaB_2	−0.21	0.25	0.04	<0.05	0.02[d]

[a]Reference 28.
[b]Reference 8.
[c]Reference 29.
[d]Reference 30.
[e]Under pressure 10 GPa.

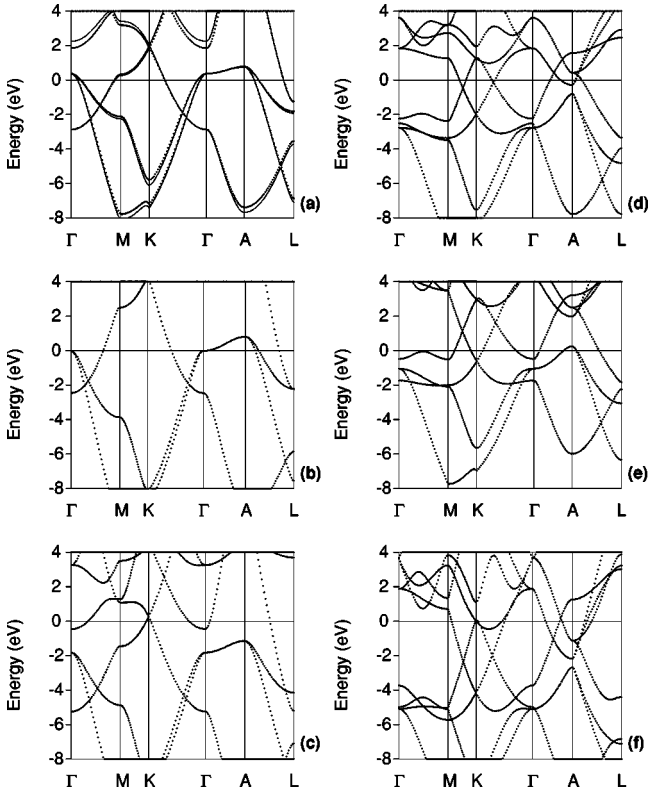

FIG. 1. Band structures of (a) MgB_2 (dotted lines for zero pressure, solid lines for 10 GPa), (b) BeB_2, (c) AlB_2, (d) TiB_2, (e) ScB_2, and (f) TaB_2.

tration, and Hopfield parameter under pressure. These investigations are of interest, since the pressure dependence of the T_c is the key difference between the conventional BCS (Ref. 3) and hole[17] superconductivity mechanisms.

The band structures of MgB_2 and some other diborides are shown in Fig. 1. There are two distinct sets of B $2p$ bands: $\sigma\,(2p_{x,y})$ and $\pi\,(p_z)$ types with considerably different dispersions. The B $2p_{x,y}$ bands are quasi-2D along the Γ-A line in the Brillouin zone (BZ) and make a considerable contribution to the density of states at the Fermi level, $N(E_F)$, for MgB_2. Now it has been shown[3–7] that the existence of degenerate $p_{x,y}$ states above E_F at the Γ point in the BZ is crucial for MTSC in diborides. The high T_c is explained by the strong coupling of these holes to the in-plane E_{2g} phonon modes.[6,18] The B $2p_z$ bands are responsible for the weaker pp_π interactions and these 3D-like bands have maximum dispersion along Γ-A. The bonding and antibonding B p_z bands cross E_F at the K point, and their location and dispersion depend on the M-B hybridization. For BeB_2 [Fig. 1(b)] and AlB_2 [Fig. 1(c)], the $p_{x,y}$ bands are, respectively, partly and completely filled, the Fermi surface topology changes, and medium-T_c superconductivity is absent.[19,20] The p_z bands progressively move down in going from BeB_2 to MgB_2 and AlB_2, demonstrating the strengthening of M-B bonding.

The band structure and chemical bonding of all $3d$-, $4d$-, and $5d$-metal diborides were previously investigated in detail.[21–24] These studies showed that the cohesive properties of AlB_2-type diborides are explained in terms of the band filling. The Fermi level for TiB_2 (ZrB_2 and HfB_2) falls in the pseudogap where bonding states are occupied and antibonding states are empty [Fig. 1(d)]. The shift of E_F results in the partial emptying of the bonding states [ScB_2, Fig. 1(e)] or the occupation of antibonding states (VB_2, CrB_2, MoB_2, TaB_2). Both cases correspond to the lowering of the cohesive properties (melting temperature, enthalpies of formation, etc.). From first-principles estimates of M-M, M-B, and B-B bonding strengths, we found that the cohesive energy of d-diborides with filled bonding states decreases when the atomic number increases in the row due to the weakening of M-B hybridization and that the AlB_2-type diborides of the group-VII and -VIII elements are unstable.[21–24] Thus the main feature of the band structure of transition-metal (TM) diborides is the progressive filling of B $p_{x,y}$, p_z bands and the dominant role of d states near E_F.

A systematic search for superconductivity in the d-diborides (with M=Ti, Zr, Hf, V, Ta, Cr, Mo) showed that T_c is below $\sim$0.4 K.[25] Only NbB_2 and ScB_2 were found to be superconductors with a T_c of about 0.6 K (Ref. 25) and 1.5 K (Ref. 26), respectively. Recently, a relatively high critical temperature $T_c \sim 9$ K was found in TaB_2.[27] As seen in Fig. 1(f), the bonding states in TaB_2 are fully occupied, the Fermi level is shifted away from the pseudogap to the region of antibonding states, and Ta $5d$ states define $N(E_F)$ (0.9 states/eV). Among the $3d$-diborides, only in ScB_2 are the $2p_{x,y}$ bands not completely filed (there is a small hole concentration of these states at A), but they lie below E_F at Γ and the largest contribution to $N(E_F)$ arises from Sc $3d$ states. Based on the band structure results and calculations of the electron-phonon interaction,[18] one may conclude that superconductivity with medium T_c is unlikely in undoped diborides, except for MgB_2; the absence of holes in the two-dimensional σ bands at Γ results in hardening of zone-phonon modes and weak electron-phonon coupling.

The electric field gradient tensor, defined as the second derivative of the electrostatic potential at the nucleus, was calculated directly from the FLMTO charge density. The calculated principal components of the boron EFG tensor, V_{zz}^B, are shown together with other theoretical and experimental data in Table I. Note that the asymmetry parameter $(|V_{xx}|-|V_{yy}|)/|V_{zz}|$ is equal to 0 for the AlB_2-type structure.

The largest boron EFG's in MgB_2 and BeB_2 demonstrate the strongest asymmetry of the charge distribution as compared with other diborides (note that here and below we consider the absolute value of EFG's). For the $3d$-diborides, the EFG decreases from ScB_2 to TiB_2 and increases when going from TiB_2 to VB_2 and CrB_2. The boron EFG's for $4d$ (MoB_2) and $5d$ (TaB_2) diborides are much smaller than the EFG's for isoelectronic $3d$-diborides. Note that all calculated EFG's are in very good agreement with available experimental data and with full-potential linearized augmented plane-wave (FLAPW) theoretical results[28] (Table I).

To analyze the variation of the boron EFG's in diborides, we consider it as a sum of electron ($V_{zz}^{\rm el}$) and lattice (ion) ($V_{zz}^{\rm lat}$) contributions (Table I). For the s,p-diborides, the ion contribution is relatively small, and the boron EFG is mainly determined by the anisotropy of the valence electrons. For

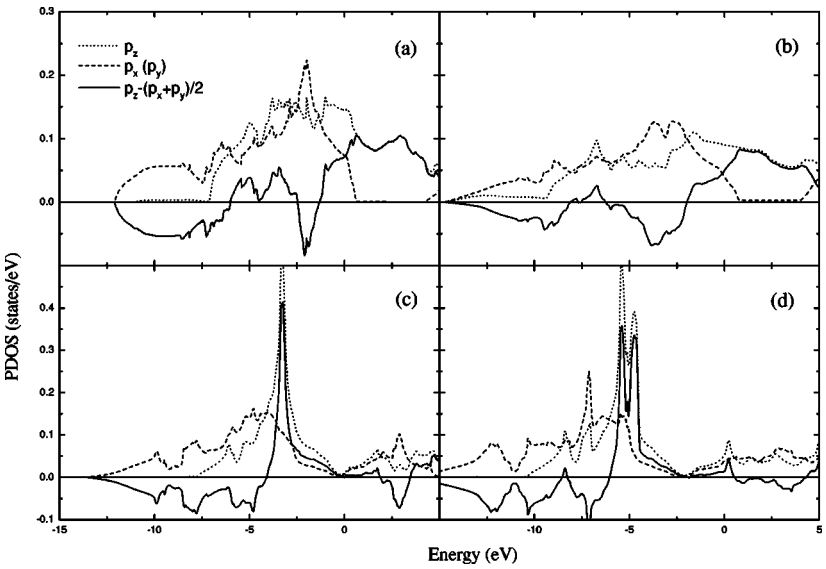

FIG. 2. Boron partial densities of $p_{x,y}$ (dashed lines) and p_z (dotted lines) states (PDOS) and their anisotropy (solid lines) for (a) MgB_2, (b) BeB_2, (c) TiB_2, and (d) TiB_2. The Fermi level corresponds to the zero energy.

the *d*-diborides, V_{zz}^{lat} is larger and depends somewhat on the metal (except ScB_2 where the lattice parameters are the largest). For TaB_2, the electron and ion contributions are almost equal: the EFG is positive and smallest among all diborides. The electronic contributions explain the boron EFG variation, although they overestimate the calculated and observed EFG's; clearly, the lattice contributions must be taken into account in order to obtain good agreement with experiment for *d*-diborides. Among the diborides, the lattice contribution is the smallest for MgB_2 and the strong charge anisotropy in MgB_2 is completely defined by the valence B *p* electrons—a property which sets MgB_2 apart from other diborides.

A qualitative explanation of EFG behavior may be given based on the anisotropy of B $2p$ partial occupancies, $\Delta n_p = p_z - (p_x + p_y)/2$, since $V_{zz}^{\mathrm{el}} \sim \langle 1/r^3 \rangle \Delta n_p$ and one may consider the boron $p\langle 1/r^3 \rangle$ expectation value to be constant for all diborides discussed. Thus the variation of the electronic EFG's is determined by the interplay of p_z and p_x, p_y occupations. As seen from the partial density of states (PDOS) obtained by means of a Mulliken population analysis, the $p_{x,y}$ orbitals are more occupied than are p_z orbitals (Fig. 2) and V_{zz}^{el} is negative for all diborides considered. For MgB_2 and BeB_2, the high-$p_{x,y}$ peaks lying below -2 eV lead to large negative Δn_p values and, therefore, to large boron EFG's. The small increase of p_z occupancy explains the EFG lowering for MgB_2 (and AlB_2) as compared to BeB_2. Thus the weaker *M*-B bonds for *s*- and *p*-diborides correspond to larger boron EFG's.

For *d*-diborides, the p_z PDOS is more localized due to strong covalent *M* $3d$-B $2p$ bonding and the high peak at 3–5 eV below E_F decreases Δn_p and V_{zz}^{el} compared with *s*- and *p*-diborides. Among the $3d$-diborides, the EFG is smallest for TiB_2, which has the strongest *p*-*d* hybridization. Weaker *p*-*d* hybridization (less intense p_z peak) for ScB_2 and CrB_2 results in a larger anisotropy Δn_p, and the boron EFG's are larger for these compounds than for TiB_2. Since $4d$ and $5d$ states are less localized than are $3d$ states, the corresponding B p_z PDOS are broadened for MoB_2 and especially for TaB_2 (Fig. 2) (the strong hybridization of B $2p$ and Ta $5d$ states was shown also in Ref. 31), which leads to the small EFG's. While a Mulliken analysis is not an accurate approach for the calculation of orbital charges, especially for delocalized *p* orbitals, it still allows one to describe general trends in EFG's and to correlate them with peculiarities of the electronic structure. Thus we conclude that *M*-B *p* hybridization is the main factor controlling the boron EFG variation.

The effect of hydrostatic pressure on the EFG at the B site in MgB_2 was investigated for 5 and 10 GPa with lattice parameters taken from the extrapolation formula[16] $a = a_0(1 - 0.00187P)$ and $c = c_0(1 - 0.00307P)$. We found a very slow increase of EFG with pressure (Table I), which also demonstrates that the boron EFG's in diborides do not have a strong dependence on the interatomic distances. As the EFG is a very sensitive characteristic, no large changes are expected in the anisotropy of the B charge distribution under pressure.

As expected, the boron *p* bands widen under pressure [Fig. 1(a)]. One can see that the band shifts relative to E_F are different for different directions of the BZ; the main changes in the occupied $p_{x,y}$ and p_z bands occur in the low-energy range at the *M*, *K*, and *A* points. These bands move down with pressure relative to E_F along Γ-*M*-*K*-Γ and *A*-*L*, and the overall shift of the PDOS to lower energies leads to the loss of these states in the energy range from E_F to -2 eV, as stated in Ref. 13. The decrease of $p_{x,y}$ and p_z PDOS near E_F is partly compensated by its increase at lower energies, and as a result, the changes in the partial *p* occupations are small. We found the increase of *p* occupancies with pressure to be anisotropic—the larger growth of $p_{x,y}$ occupancy compared to p_z giving an Δn_p increase by 0.02 of 10 GPa. An accurate calculation gives a smaller EFG than follows from Δn_p. As seen from Table I, the increase of B *p*-electron anisotropy is partly compensated by the increase of the core charge contribution, and as a result, the boron EFG in MgB_2 is weakly dependent on applied pressure. Thus we conclude that the charge distribution at the B site shows more isotropic change under pressure than do the B *p* valence electrons due to the

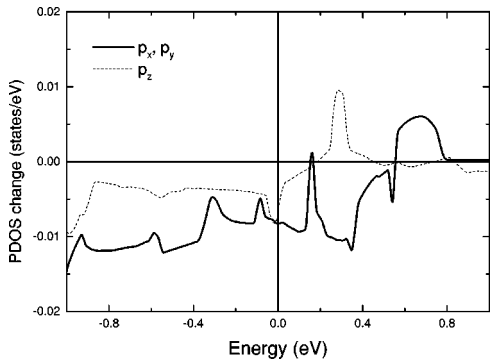

FIG. 3. The change in the boron $p_{x,y}$ (solid lines) and p_z (dashed line) PDOS in MgB_2 under a pressure of 10 GPa. The Fermi level corresponds to the zero energy.

compensating behavior of electron and core systems. NMR measurements under pressure would be important to confirm this conclusion.

The PDOS changes near E_F under a pressure of 10 GPa are shown in Fig. 3. The hole concentration in the bonding σ bands decreases by 0.005 (within an energy interval up to 0.8 eV). The changes in $p_{x,y}$ PDOS are due to the behavior of these bands with pressure along Γ-A: the bands move down at Γ and up at A, resulting, respectively, in the loss of holes in the energy range up to 0.5 eV and their increase for higher energies. Although the hole p_z PDOS change is negative in the energy interval up to 0.2 eV, its concentration is almost constant under pressure for energies up to 0.8 eV. The loss of both $p_{x,y}$ and p_z states near E_F results in a small decrease of $N(E_F)$ by 0.02 states/eV. Thus we showed that the carrier concentration decreases, and so the observed decrease of the resistance with pressure is likely to be connected with better coupling between the sintered grains, as suggested in Ref. 33.

Finally, we estimated the pressure dependence of the Hopfield parameter η, which is an electronic part of the electron-phonon coupling $\lambda = \eta / M\langle\omega^2\rangle$, where $\eta = N(E_F)\langle I^2\rangle$. The calculation of the averaged electron-ion matrix element squared $\langle I^2\rangle$, performed within the rigid muffin tin approximation,[32] gave a faster increase of $\langle I^2\rangle$ with pressure than the $N(E_F)$ decrease. As a result, despite a small decrease of $N(E_F)$, $(dN(E_F)/dP = -0.51\%/\mathrm{GPa})$, the Hopfield parameter increases with pressure as $d\eta/dP = +0.55\%/\mathrm{GPa}$. Hence the decrease of $N(E_F)$ cannot be considered as the reason for the T_c reduction, which is known[34] to behave as $dT_c/dP = -1.6\,\mathrm{K/GPa}$. Thus, according to the McMillan formula, the main reason for the reduction of T_c under pressure is the strong pressure dependence of phonon frequencies, which is sufficient to compensate for the electronic effects.

Work at Northwestern University was supported by the U.S. Department of Energy (Grant No. DF-F602-88ER45372).

[1] J. Akimitsu (unpublished); J. Nagamatsu *et al.*, Nature (London) **410**, 63 (2001).
[2] A. L. Ivanovskii and N. I. Medvedeva, Russ. J. Inorg. Chem. **45**, 1234 (2000).
[3] J. Kortus, I. I. Mazin, K. D. Belashenko, V. P. Antropov, and L. L. Boyer, Phys. Rev. Lett. **86**, 4656 (2001).
[4] K. D. Belashchenko, M. van Schilfgaarde, and V. P. Antropov, Phys. Rev. B **64**, 092503 (2001).
[5] G. Satta, G. Profetta, F. Bernardini, A. Continenza, and S. Massidda, Phys. Rev. B **64**, 104507 (2001).
[6] J. M. An and W. E. Pickett, Phys. Rev. Lett. **86**, 4366 (2001).
[7] N. I. Medvedeva, A. L. Ivanovskii, J. E. Medvedeva, and A. J. Freeman, Phys. Rev. B **64**, 020502 (2001).
[8] A. Gerashenko *et al.*, cond-mat/0102421 (unpublished).
[9] H. Kotegawa, K. Ishida, Y. Kitaoka, T. Muranaka, and J. Akimitsu, Phys. Rev. Lett. **87**, 127001 (2001).
[10] S. L. Bud'ko, G. Lapertot, C. Petrovic, C. E. Cunningham, N. Anderson, and P. C. Canfield, Phys. Rev. Lett. **86**, 1877 (2001).
[11] M. Methfessel and M. Scheffler, Physica B **172**, 175 (1991).
[12] I. Loa and K. Syassen, Solid State Commun. **118**, 279 (2001).
[13] T. Vogt, G. Schneider, J. A. Hriljac, G. Yang, and J. S. Abell, Phys. Rev. B **63**, 220505 (2001).
[14] A. K. M. A. Islam, F. N. Islam, and S. Kabir, J. Phys.: Condens. Matter **13**, L641 (2001).
[15] P. Ravindran *et al.*, cond-mat/0104253 (unpublished).
[16] J. D. Jorgensen, D. G. Hinks, and S. Short, Phys. Rev. B **63**, 4222 (2001).
[17] J. E. Hirsh, Phys. Lett. A **282**, 392 (2001).
[18] Y. Kong, O. V. Dolgov, O. Jepsen, and O. K. Andersen, Phys. Rev. B **64**, 020501 (2001).
[19] I. Felner, Physica C **353**, 1 (2001).
[20] J. S. Slusky *et al.*, Nature (London) **411**, 6833 (2001).
[21] A. L. Ivanovskii, N. I. Medvedeva, J. E. Medvedeva, and A. E. Nikiforov, Metallofiz. Noveishie Tekhnol. **20**, 41 (1998).
[22] A. L. Ivanovskii, N. I. Medvedeva, and J. E. Medvedeva, Metallofiz. Noveishie Tekhnol. **21**, 19 (1999).
[23] A. L. Ivanovskii, N. I. Medvedeva, and J. E. Medvedeva, Mendeleev Commun. **4**, 129 (1998).
[24] A. L. Ivanovskii, N. I. Medvedeva, and J. E. Medvedeva, Dokl. Akad. Nauk **361**, 642 (1998).
[25] L. Leyarovska and E. Leyarovski, J. Less-Common Met. **67**, 249 (1979).
[26] G. V. Samsonov and I. M. Vinitsky, *Refractory Compounds* (Metallurgija, Moskva, 1976).
[27] D. Kaczorowski *et al.*, cond-mat/0103571 (unpublished).
[28] K. Schwarz, H. Ripplinger, and P. Blaha, Z. Naturforsch., A: Phys. Sci. **51**, 527 (1996).
[29] J. P. Kopp and R. G. Barnes, J. Chem. Phys. **54**, 1840 (1971).
[30] A. H. Silver and T. Kushida, J. Chem. Phys. **38**, 865 (1963).
[31] H. Rosner *et al.*, Phys. Rev. B **64**, 144516 (2001).
[32] For zero pressure we obtained the Hopfield parameter $\eta = 129.2\,\mathrm{mRy}/a_B^2$, which is very close to value $135\,\mathrm{mRy}/a_B^2$ from Ref. 3 and leads to approximately the same $T_c \sim 20\,\mathrm{K}$ for the Coulomb pseudopotential $\mu = 0.1$ and phonon frequency $\langle\omega_{\log}\rangle = 500\,\mathrm{cm}^{-1}$.
[33] M. Monteverde *et al.*, Science **292**, 75 (2001).
[34] B. Lorentz, R. L. Meng, and C. W. Chu, Phys. Rev. B **64**, 012507 (2001).